Modeling High Energy Density Electrical Inductors Operating at THz Frequencies Based on Coiled Carbon Nanotubes

Hasan Mohammad Faraby, Apparao M. Rao, and Prabhakar R. Bandaru

***Abstract*— We propose the use of coiled carbon nanotubes (CCNTs) as nanoscale electrical inductor elements, inspired by the paradigm of function follows form. We show through computations that a range of inductance values (in the pH to μH) operational at terahertz frequencies could be obtained through a variation of CCNT geometric parameters, which can be accomplished through rational synthesis. A comparison of the proposed inductor material to conventional inductor material e.g., copper, in terms of both component footprint and material volume, indicate a greater quality factor ($Q = \omega L/R$) through the use of the CCNTs.**

***Index Terms*— Coiled carbon nanotube (CCNT), kinetic inductance, quality factor, self-resonant frequency.**

I. Introduction

OF THE three fundamental components of electrical circuits, i.e., resistors, capacitors, and inductors, there was negligible change in the design of the latter over the past 40 years [1]. Therefore, inductors, which are integral to a variety of power electronics, radio frequency, microwave, and analog/mixed signal applications, are widely considered [1] to be expensive and bulky elements, not easily amenable to scaling down at high power and frequency. The purpose of this letter is then to suggest that rationally synthesized coiled carbon nanotubes (CCNTs) may be used for high performance inductors, while maintaining small component footprint. The detailed synthesis procedures and mechanisms of formation were reported previously [2]. The performance characteristics of inductors may be parameterized through three attributes: 1) their magnitude (L); 2) the quality factor, $Q(=\omega L/R)$, at a given operating frequency (f), where ω $(=2\pi f)$ and R is the intrinsic/parasitic resistance; and 3) the self-resonant frequency, f_{SR} $(=1/(2\pi\sqrt{LC}))$ with C as the parasitic capacitance. Although Q is inversely proportional to the power loss in an inductor, f_{SR} is the highest operating frequency, i.e., for $f > f_{SR}$, the parasitic capacitance is dominant. The parasitic resistance could arise as a result of: 1) dc resistance; in addition to frequency-dependent contributions from; 2) skin effect; and 3) eddy currents and dielectric losses from the substrate. To reduce the dc component, conventional copper based on chip inductors presently utilize a thick metal layer [3]. The influence of skin effect is pernicious, in enhancing parasitic resistance, in conventional inductors at higher frequencies (where the skin depth is in the order of 400 nm at ~40 GHz). Therefore, investigation of the characteristics of inductor materials, at the nanoscale, where such parasitic effects could be minimized would be relevant and interesting. We will then show the potential of CCNTs to drastically reduce the limitations of conventional inductors extending operating frequencies up to 10 THz. The foundation is their superior current carrying capacity with low electrical resistance and negligible parasitic because of coiled geometry, along with the harness of the kinetic inductance (L_k) in addition to electromagnetic inductance (L_{em}). Moreover, an individual atomic layer thick CNT/graphene sheets would not be susceptible to skin effect.

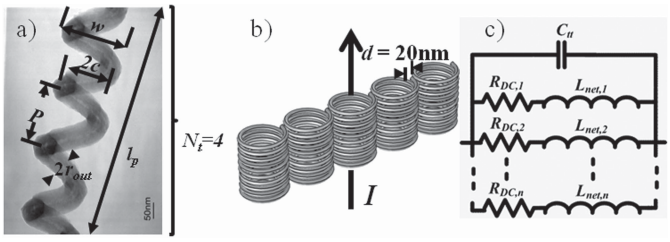

Fig. 1. (a) SEM image of a CCNT denoting width (w), outer tube radius (r_{out}), pitch (P), coil radius (c), projected length (l_p), and number of turns (N_t). (b) Geometry of a five CCNT bundle, each of them has $r_{out} = 10$ nm, $c = 100$ nm, $P = 30$ nm, and $N_t = 10$, spacing between adjacent CCNT is 20 nm. The direction of current flow is shown with the arrow. (c) Proposed equivalent circuit of a CCNT with n shells for f_{SR} calculation. One and n are the outermost and innermost shell.

II. Computational Details

We model the CCNT as metallic multiwall CNT with the following four geometric parameters shown in Fig. 1(a), i.e.: 1) tube radius, r; 2) coil radius, c; 3) pitch, P; and 4) number of turns, N_t. When electrical current (I) is passed, the electromagnetic inductance (L_{em}) would comprise contributions from flux linkage interior and exterior to the CCNT, i.e.,

Manuscript received February 17, 2013; revised March 26, 2013; accepted April 13, 2013. Date of publication May 13, 2013; date of current version May 20, 2013. This work was supported by the National Science Foundation under Grant ECS 0643761. The review of this letter was arranged by Editor William S. Wong.

H. M. Faraby is with the Electrical and Computer Engineering Department, University of California, San Diego, CA 92093 USA.

A. M. Rao is with the Department of Physics and Astronomy, Clemson University, Clemson, SC 29634 USA.

P. R. Bandaru is with the Department of Mechanical Engineering, University of California, San Diego, CA 92093 USA (e-mail: pbandaru@ucsd.edu).

Color versions of one or more of the figures in this paper are available online at http://ieeexplore.ieee.org.

Digital Object Identifier 10.1109/LED.2013.2258454

$L_{M,int}$ and $L_{M,ext}$, respectively. The CCNT is modeled as a tube with an inner and outer radius ($r_{in} = 5$ nm and $r_{out} = 10$ nm) as in Fig. 1(a), with an extended/total length, l_t and an coiled/projected length, l_p, and the inductances/unit length are estimated (assuming the CCNT to be akin to a long solenoid [4], as l_p is typically much more than three times c) through

$$L_{M,int} = \left(\frac{\mu}{2\pi(r_{out}^2 - r_{in}^2)^2}\right) \cdot \left[\frac{r_{out}^4 - r_{in}^4}{4} - r_{in}^2(r_{out}^2 - r_{in}^2) + r_{in}^4 \ln\left(\frac{r_{out}}{r_{in}}\right)\right] \quad (1)$$

$$L_{M,ext} = (\pi \mu c^2 N_t^2)/l_p^2. \quad (2)$$

The results obtained by (1) and (2) are confirmed by numerical simulations using COMSOL Multiphysics, where Maxwell's equations are solved to determine the impedance of a CCNT with $r_{out} = 10$ nm, $c = 100$ nm, $P = 30$ nm, and $N_t = 10$. In addition, the f_{SR} of the CCNT structures are ~25 THz from a full wave electromagnetic simulation using high frequency structure simulator. A substantially additional contribution, to the net inductance, would be from the constituent 1-D single-wall nanotubes (SWNTs) through their kinetic inductance (L_k) [5], which arises because of a consideration of inherent electronic motion [6]. The underlying idea is that the flux loops formed through forward and backward electronic propagation would yield an inductance: L_k. Considering that each electronic channel of conduction would contribute to L_k, we enumerate the total number of contributing channels (N_{chan}) for a given CCNT diameter. This may be done through counting the number of occupied modes (M) for a single constituent SWNT and then summing over the multiple SWNTs (m) that comprise the CCNT through

$$N_{chan} = \sum_{i}^{m} \sum_{j}^{M} f_j \quad (3)$$

where $f_j (= 1/(\exp(|E_j - E_F|/k_B T) + 1))$ is the Fermi–Dirac function and is a measure of the number of occupied energy levels. The m would be proportional to the r_{out}, and therefore a relationship of the form

$$N_{chan} = a \cdot r_{out} + b \quad (4)$$

with $a = 0.1224$ nm^{-1} and $b = 0.425$ could be fitted [7]. The L_k/unit length can then be derived to be $h/(4v_F e^2 N_{chan})$, where h is the Planck constant, v_F is the Fermi velocity, and e is the elementary electronic charge. This relation of L_k is experimentally proved for SWCNTs for frequencies > 10 GHz [8] and previous simulations [9] have shown negligible dependence of $L_k > 200$ GHz. Therefore, the net inductance, L_{net} (incorporating both classical and quantum effects) can be expressed as follows:

$$L_{net} = l_t \cdot L_{M,int} + l_p \cdot L_{M,ext} + l_t \cdot L_k \quad (5)$$

and plotted as a function of r_{out} and c in Fig. 2. L_{net} may be tuned by orders of magnitude through varying r_{out} and c. A thinner tube (smaller r_{out}) is more effective in enhancing the inductance in that the effective flux loop area would be increased (for an equivalent I). However, the component footprint area, A [product of $l_p (= P \cdot N_t)$ and width, $w (= 2(r_{out} + c))$, Fig. 1(a)] is still diminished. The variation of L_{net} with P is found to be insignificant.

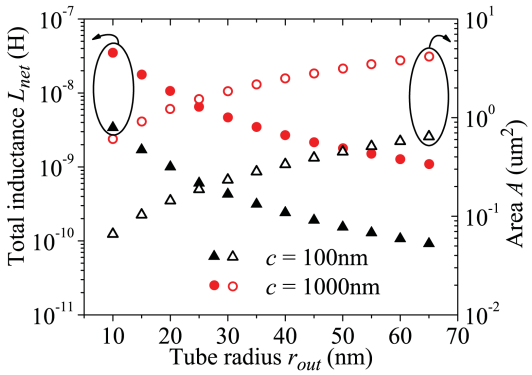

Fig. 2. L_{net} and A versus r_{out} at $c = 100$ and 1000 nm, $P = 3r_{out}$, and $N_t = 10$.

In addition to tunability of L_{net} and reduced A, we have also seen that other important attributes such as f_{SR} and Q could be enhanced over conventional inductors. Presently, f_{SR} of inductors is limited to ~40 GHz [10] because of large parasitic capacitance brought about by component overlap and interaction with substrate. However, with CCNTs, f_{SR} values of the order of 10 THz may be achieved because of substantially reduced parasitic capacitance. The individual shells of the CCNT are coupled capacitively through quantum capacitance (C_q) as well as electrostatically (C_{es}) arising from varying voltage distributions in the shells, but such capacitances do not contribute to f_{SR} because of shielding from the outer most shell. Only C_q and C_{es} of the outermost shell contributes to f_{SR}, but C_{es} (which is in series with and typically smaller [11] than C_q) from the outermost shell can be ignored as ideally the circular coils will touch the substrate to a point (as a tangent) essentially making the parasitic capacitance from the substrate negligible as capacitance varies directly with overlapped area. The capacitance, which does contribute to f_{SR} is the equivalent capacitance that arises because of the interaction between adjacent turns of the coil, i.e., $C_{tt} (= C_t/(N_t - 1))$. We calculate C_{tt} as 1.8 aF, which is a series combination of capacitance between adjacent turns, C_t, we calculate C_t neglecting the turn curvature, therefore, they can be modeled as two infinitely long parallel wires in a homogenous medium separated by P and we also assume the capacitance between nonadjacent turns to be negligible as they are relatively far from each other. This method is experimentally verified for single-layer solenoid air-core inductors [12]. Using these assumptions, the equivalent circuit for obtaining f_{SR} is shown in Fig. 1(c) where each shell of the CCNT is modeled as series combination of L_{net} and R_{DC} [incorporating resistance because of both quantum effects, $R_q (= h/2e^2 N_{chan})$] and scattering, $R_s (= (hl_t)/(2e^2 N_{chan} \lambda))$, where λ ($\sim 2000\, r_{out}$) is the mean free path [13]). We calculate $R_{DC} \sim 1.2$ kΩ (with $r_{out} = 10$ nm, $c = 100$ nm, $P = 30$ nm, and $N_t = 10$). Thus, we consider all the quantum and classical

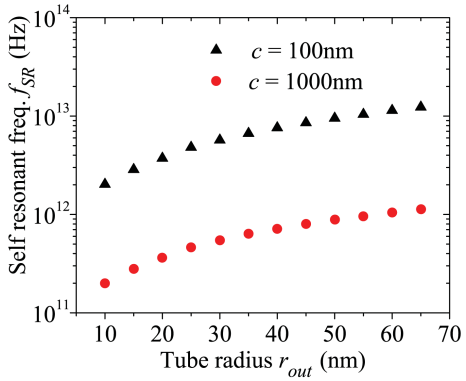

Fig. 3. f_{SR} versus r_{out} at $c = 100$ and 1000 nm for $P = 3r_{out}$, and $N_t = 10$ using the equivalent circuit from Fig. 1(c).

TABLE I
COMPARISON OF L/R_{DC} OF CCNT BUNDLE (MATLAB) AND EQUIVALENT CU BLOCK (FASTHENRY2)

Bundle of CCNT	Equivalent Footprint (Cu)	Equivalent Material (Cu)
$L \sim 680$ pH	$L \sim 0.03$ pH	$L \sim 0.081$ pH
$R_{DC} \sim 240\ \Omega$	$R_{DC} \sim 0.02\ \Omega$	$R_{DC} \sim 0.21\ \Omega$
$L/R_{DC} \sim 3$ pH/Ω	$L/R_{DC} \sim 1.5$ pH/Ω	$L/R_{DC} \sim 0.39$ pH/Ω

effects that are dominant in our CCNT structure as intershell tunneling is found to be insignificant [14]. Our model yields f_{SR} values in the order of 1 THz or greater (Fig. 3).

To analyze the energy efficiency we compare the Q of a bundle of CCNTs (Fig. 1(b), each of which have the same dimensions as above) with a 20-nm separation between adjacent CCNTs with a conventional inductor material e.g., copper (Cu), of equivalent: 1) component footprint volume and 2) actual material volume. As, we propose to use parallel arrays of the CCNTs (because of reduced resistance), five CCNTs are considered representative for comparison with prevalent inductor section (which typically have widths in the range of 1–10 μm [15]). We consider both L_{net} and their mutual inductance (M_{ij}) (because of the interaction of magnetic flux among neighboring CCNTs) for each CCNT in the bundle. For obtaining M_{ij} we model the CCNTs as solenoids with parallel axes [16]. Therefore, the overall impedance of each CCNT in the bundle will contain self-impedance, $Z_{nn}(= R_{DC} + j\omega L_{net})$ and four mutual impedance terms for its four neighbors. Applying Ohm's law for all the CCNTs in the bundle we obtain a system of five linear equations as follows:

$$\begin{bmatrix} V_1 \\ V_2 \\ V_3 \\ V_4 \\ V_5 \end{bmatrix} = \begin{bmatrix} Z_{11} & M_{12} & M_{13} & M_{14} & M_{15} \\ M_{21} & Z_{22} & M_{23} & M_{24} & M_{25} \\ M_{31} & M_{32} & Z_{33} & M_{34} & M_{35} \\ M_{41} & M_{42} & M_{43} & Z_{44} & M_{45} \\ M_{51} & M_{52} & M_{53} & M_{54} & Z_{55} \end{bmatrix} \begin{bmatrix} I_1 \\ I_2 \\ I_3 \\ I_4 \\ I_5 \end{bmatrix} \quad (6)$$

where the mutual inductance terms obtained from Grover [16] is expressed as $M_{ij}(= j\omega L_{m,ij}, i, j = 1, 2, \ldots, 5)$ and $V_1 = V_2 = V_3 = V_4 = V_5 = V$, as all the CCNTs in the bundle are identical. We solve (6) for a wide range of currents (1 nA–1 mA) to obtain V. Using V and total current, $I_T(= I_1 + I_2 + I_3 + I_4 + I_5)$ through the CCNT bundle we can compute the equivalent impedance (Z_{eff}) of the bundle, the imaginary part of $Z_{eff}(= V/I_T = R_{eff} + j\omega L_{eff})$ will give us the effective inductance (L_{eff}) of the bundle. This L_{eff} of the CCNT bundle is used in Table I and compared with the inductance of above described section of conventional inductor material.

III. CONCLUSION

We suggested that CCNTs could be used as a novel type of inductor element. We initiated experimental investigations to verify our calculations and obtained preliminary results indicating reasonable agreement with predictions.

ACKNOWLEDGMENT

The authors would like to thank S. Pfeifer and M. Dibattista (Qualcomm Inc.) for their support.

REFERENCES

[1] R. Ram, "Power electronics," presented at the Power Electronics, ARPA-E Workshop, Washington, DC, USA, 2010.

[2] P. R. Bandaru, C. Daraio, K. Yang, and A. M. Rao, "A plausible mechanism for the evolution of helical forms in nanostructure growth," *J. Appl. Phys.*, vol. 101, no. 9, pp. 094307-1–094307-4, 2007.

[3] *International Technology Roadmap for Semiconductors*, Semiconductor Industry Association (SIA) *et al.*, Washington, DC, USA, 2011.

[4] S. Ramo, J. R. Whinnery, and T. van Duzer, *Fields and Waves in Communication Electronics*, 3 ed. New York, NY, USA: Wiley, 1993.

[5] W. Wang, S. Haruehanroengra, L. Shang, and M. Liu, "Inductance of mixed carbon nanotube bundles," *IET Micro Nano Lett.*, vol. 2, no. 2, pp. 35–39, Jun. 2007.

[6] P. R. Bandaru, "Electrical properties and applications of carbon nanotube structures," *J. Nanosci. Nanotechnol.*, vol. 7, nos. 4–5, pp. 1239–1267, 2007.

[7] A. Naeemi and J. D. Meindl, "Compact physical models for multiwall carbon nanotube interconnects," *IEEE Electron Device Lett.*, vol. 27, no. 5, pp. 338–340, May 2006.

[8] J. J. Plombon, K. P. O'Brien, F. Gstrein, V. M. Dubin, and Y. Jiao, "High-frequency electrical properties of individual and bundled carbon nanotubes," *Appl. Phys. Lett.*, vol. 90, no. 6, pp. 063106-1–063106-3, 2007.

[9] L. Hong and K. Banerjee, "High-frequency effects in carbon nanotube interconnects and implications for on-chip inductor design," in *Proc. IEEE Int. Electron Devices Meeting*, Dec. 2008, pp. 1–4.

[10] J. Kim, B. Nam, and H. Kim, "A new differential stacked spiral inductor with improved self-resonance frequency," *Microw. Opt. Technol. Lett.*, vol. 53, no. 5, pp. 1024–1026, 2011.

[11] P. J. Burke, "Luttinger liquid theory as a model of the gigahertz electrical properties of carbon nanotubes," *IEEE Trans. Nanotechnol.*, vol. 1, no. 3, pp. 129–144, Sep. 2002.

[12] G. Grandi, M. K. Kazimierczuk, A. Massarini, and U. Reggiani, "Stray capacitances of single-layer solenoid air-core inductors," *IEEE Trans. Ind. Appl.*, vol. 35, no. 5, pp. 1162–1168, Sep.–Oct. 1999.

[13] H. Li, W.-Y. Yin, K. Banerjee, and J.-F. Mao, "Circuit modeling and performance analysis of multi-walled carbon nanotube interconnects," *IEEE Trans. Electron Devices*, vol. 55, no. 6, pp. 1328–1337, Jun. 2008.

[14] B. Bourlon, C. Miko, L. Forró, D. C. Glattli, and A. Bachtold, "Determination of the intershell conductance in multiwalled carbon nanotubes," *Phys. Rev. Lett.*, vol. 93, no. 17, pp. 176806-1–176806-4, 2004.

[15] D. S. Gardner, G. Schrom, F. Paillet, B. Jamieson, T. Karnik, and S. Borkar, "Review of on-chip inductor structures with magnetic films," *IEEE Trans. Magn.*, vol. 45, no. 10, pp. 4760–4766, Oct. 2009.

[16] F. W. Grover, *Inductance Calculations*. New York, NY, USA: Dover, 2009.